The American Journal of Pathology, Vol. 173, No. 5, November 2008

DOI: 10.2353/ajpath.2008.080056

Cardiovascular, Pulmonary and Renal Pathology

A Mutation in Rab38 Small GTPase Causes Abnormal Lung Surfactant Homeostasis and Aberrant Alveolar Structure in Mice

Kazuhiro Osanai,* Rieko Oikawa,* Junko Higuchi,† Makoto Kobayashi,* Katsuma Tsuchihara,* Masaharu Iguchi,* Huang Jongsu,* Hirohisa Toga,* and Dennis R. Voelker‡

From the Department of Respiratory Medicine, Kanazawa Medical University, Ishikawa, Japan; Department of Human Pathology,† Yamagata University Graduate School of Medicine, Yamagata, Japan; and Program in Cell Biology,‡ National Jewish Medical and Research Center, Denver, Colorado*

The *chocolate* mutation, which is associated with oculocutaneous albinism in mice, has been attributed to a G146T transversion in the conserved GTP/GDP-interacting domain of Rab38, a small GTPase that regulates intracellular vesicular trafficking. Rab38 displays a unique tissue-specific expression pattern with highest levels present in the lung. The purpose of this study was to characterize the effects of Rab38-G146T on lung phenotype and to investigate the molecular basis of the mutant gene product (Rab38^{cbt} protein). Chocolate lungs exhibited a uniform enlargement of the distal airspaces with mild alveolar destruction as well as a slight increase in lung compliance. Alveolar type II cells were engorged with lamellar bodies of increased size and number. Hydrophobic surfactant constituents (ie, phosphatidylcholine and surfactant protein B) were increased in lung tissues but decreased in alveolar spaces, consistent with a malfunction in lamellar body secretion and the subsequent cellular accumulation of these organelles. In contrast to wild-type Rab38, native Rab38^{cbt} proteins were found to be hydrophilic and not bound to intracellular membranes. Unexpectedly, recombinant Rab38^{cbt} proteins retained GTP-binding activity but failed to undergo prenyl modification that is required for membrane-binding activity. These results suggest that the genetic abnormality of Rab38 affects multiple lysosome-related organelles, resulting in lung disease in addition to oculocutaneous albinism. *(Am J Pathol 2008, 173:1265–1274; DOI: 10.2353/ajpath.2008.080056)*

Rab38 is a member of Rab small GTPase family that regulates intracellular vesicle trafficking.[1–4] Information from both the human genome and expressed sequence tag databases predicts that the Rab family contains approximately 60 members. Rab proteins and their effectors coordinate multiple stages of membrane transport, such as vesicle formation, motility, and tethering to their target compartments. These proteins can also be found in both membrane-bound and cytosolic forms and are prenylated at their carboxyl termini. Prenyl modifications are essential for biological activity, as these signals are required for localization of Rab proteins to specific cellular organelles.

The Rab38 cDNA was originally cloned from a rat lung cDNA library (GenBank Accession No. M94043), and later from a human melanoma cDNA library.[5–6] Although many Rab proteins are ubiquitously expressed in a variety of tissues and cells, the expression of some Rab proteins (including Rab38) are selectively regulated and dependent on cell type (epithelial, neuronal, endocrine, or exocrine) and specific cell state (differentiation or polarization). Rab38 mRNA and protein are expressed predominantly in the lung, skin, stomach, liver, and kidney in rats.[7] Rab38 is specifically expressed in alveolar type II and Clara cells in rat lung tissue.[5] These lung-specific cells synthesize and secrete lung surfactant that lowers alveolar surface tension and thereby maintains alveolar lumen in an open and relatively dry state.

Chocolate (*cht*) is an autosomal recessive mutation that arose spontaneously in C57BL/6J mice.[8] The mutant mouse with its phenotype of oculocutaneous albinism was recently identified as having a point mutation in the Rab38 gene.[9] Genomic DNA analysis revealed a G146T transversion that resulted in a replacement of glycine with valine in the conserved GTP/GDP-interacting domain

Supported by Grant-in-Aid for Scientific Research (C) (2) 15590833 Japan Society for Promotion of Science and Grant for Promoted Research from Kanazawa Medical University (S2005-9).

Accepted for publication July 25, 2008.

Address reprint requests to Kazuhiro Osanai, Department of Respiratory Medicine, Kanazawa Medical University, 1-1 Uchinada-Daigaku, Kahokugun, Ishikawa 920-0293, Japan. E-mail: k-osanai@kanazawa-med.ac.jp.

near the N-terminus. Rab38 appears to participate in trafficking of melanogenic enzymes in skin melanocytes[10] and retinal pigment epithelial cells.[11] This mutation predicts a loss of GTP/GDP-binding activity and a resultant GTP/GDP molecular switch dysfunction. However, molecular characterization of the mutant gene product (Rab38^{cht}) has not been performed. Moreover, because of the high level of lung expression, it seemed probable that the chocolate mutation would also cause lung disease in addition to oculocutaneous albinism.[7] Thus, the purpose of this study was to characterize possible effects of the Rab38-G146T on phenotype of the mouse lung and to provide molecular basis of the dysfunction of the mutant gene product (Rab38^{cht} protein).

Materials and Methods

Reagents

Common chemicals were purchased from Sigma (St. Louis, MO) or Wako Chemicals (Osaka, Japan). Rabbit anti-human SP-A, anti-sheep SP-B, anti-mouse SP-D, and mouse anti-glyceraldehyde-3-phosphate dehydrogenase antibody were from Chemicon (Temecula, CA). Horseradish peroxidase-conjugated goat anti-rabbit IgG antibody and anti-mouse IgG antibody were from Bio-Rad (Hercules, CA). A chemiluminescent detection kit, a stripping buffer, and a micro-BCA protein assay kit were from Pierce (Rockford, IL). Autoradiography films and autofluorography films for Western blot analysis were from Kodak (Rochester, NY). The thin-layer chromatography apparatus was from Advantec (Tokyo, Japan), and Silica gel G plates were from Analtec (Uniplate, Newark, DE). Insect cell lines (Sf9 cells), Bac-N-Blue transfection kit, pBlueBacHis2-A plasmid, and Ni^{++}-charged affinity chromatography resin were from Invitrogen (Carlsbad, CA).

Mice

All animal protocols were reviewed and approved by the Institutional Animal Care and Use Committee in Kanazawa Medical University. Two couples of a male chocolate heterozygous (*cht*/+) mouse and a female chocolate homozygous (*cht/cht*) mouse were purchased from the Jackson Laboratory (Bar Harbor, ME). Specific-pathogen-free animals were generated by rederivation using an embryo transfer method in Japan Charles River Inc. (Yokohama, Japan). The genotypes of chocolate mice were determined by DNA sequence of PCR products of exon 1 of genomic DNA. Rab38 primer pairs were designed to amplify exon 1: Ex1F (5′-TAGGAAGGAGGATTAAACCCG-3′) and Ex1R (5′-GAACTCCTCATGGCTCACTCC-3′), yielding a 428-bp product. The chocolate mutation was confirmed by using primers designed to amplify a 213-bp fragment containing the G146T sequence: *cht* Ex1F (5′-GGCCTCCAGGATGCAGACACC-3′) and *cht* Ex1R (5′-CCAGCAATGTCCCAGAGCTGC-3′).[9]

Lung Histology

Male mice at 12 and 24 weeks old were sacrificed by severing the abdominal aorta under intraperitoneal anesthesia with sodium pentobarbital (~100 mg/kg body weight) plus sodium heparin (~3300 units/kg body weight). The lungs and heart were removed *en bloc*. The lungs were carefully inflated with 2.5% glutaraldehyde in 0.1 M cacodylate buffer (pH 7.4) at a constant hydrostatic pressure of + 25 cmH_2O at the height of the carina in the upright position. After the lung volume was measured by water displacement, the right and left lungs were separated, embedded in paraffin, and cut into 5 μm-thick sections in the sagittal plane so as to contain the largest lung area. Care was taken to cut the fixed lungs at the same thickness without any distortion. The lungs were stained using H&E.

Morphometry

An imaginary rectangle whose four sides touched the outline of a lung slice was defined on the microscope stage and was divided into more than 40 fields of the same size. Each field was photographed at 295 × 223 μm^2 and contained 35 equidistant test points; two test lines connecting the opposite angle, both 370 μm in length, were drawn on the field. Every test point was classified into one of six categories based on its histological component (alveolar air space, air space in alveolar ducts and sacs, alveolar wall, bronchial and bronchiolar wall, blood vessel wall, and other). Large airways and vessels were excluded from the analysis. The numbers of test points were summed for each of the tissue components, and the volume proportion of the defined tissue component was expressed as a proportion of the total number of points according to the point-counting method.[12] Based on the point-counting method modified by Kawakami and associates,[13] mean thickness of the alveolar wall (τw), mean linear intercept (Lm), mean chord length of alveoli (la), and mean chord length of ducts and sacs (ld) were calculated. Using another point-counting system, an index of parenchymal destructive change that represents the percentage of destroyed space as a fraction of the total alveolar and duct space, referred to as the destructive index (DI), was calculated.[14,15]

Lung physiology

Male mice at 24 weeks old were used for measurement of lung pressure-volume relationships. Mice were anesthetized by intraperitoneal injection of sodium pentobarbital (~100 mg/kg body weight). The trachea was exposed and cannulated with an 18G catheter attached to a three-way stopcock. The mice were mechanically ventilated with 100% O_2 (~0.5 ml tidal volume and ~60 cpm) (Harvard model 683, South Natick, MA) for 10 minutes, followed by 5 minutes closure of the trachea to completely degas the lungs.[16] The mice were exsanguinated and the anterior chest and diaphragm were dissected away. The lungs were attached to a syringe pump (Minato MCIP-III, Tokyo, Japan) and a semiconductor pressure transducer (Kulite XCW-190-5D, Leonia, NJ) through

the three-way stopcock, and inflated in stepwise fashion with small increments of air (0.1 ml every 20 seconds) to a maximal pressure of 25 cmH_2O. The lungs were deflated in stepwise fashion (~2.5 cmH_2O decrements every 5 seconds) down to −10 cmH_2O. This inflation-deflation cycle was repeated two times, and the third cycle was used for analysis, except for airway opening pressure that was measured from the first cycle inflation. Care was taken not to cause air leak from the lungs. When air leak was found, the lungs were discarded. Pressure-volume curves were plotted and used to assess lung compliance, which was defined as a slope of the linear region of the deflation limb where pressure ranged from 0 to 5 cmH_2O. Specific lung compliance was calculated as lung compliance divided by the lung volume at 25 cmH_2O. The hysteresis ratio was determined as described by Nardell and Brody.[16]

Electron Microscopy

Mice at 18 weeks old and 17 days fetal mice were used. The excised lungs were cut into small pieces and fixed for 2 hours with fresh fixative containing 2.5% glutaraldehyde/0.1% picric acid/2% osmium tetroxide/4% sucrose/0.1 M cacodylate buffer (pH 7.4). Blocks were post fixed with 1% aqueous uranyl acetate solution for 1 hour followed by dehydration in a graded series of ethanol and subsequent propylene oxide, and were finally embedded in Epon. Thin sections were counterstained with 2% uranyl acetate, and then 2.66% lead nitrate/3.52% sodium citrate (pH 12). The sections were examined using a Hitachi H-7100 transmission electron microscope.

Lamellar Body Isolation

Male mice at 18 weeks old were used. One ml of saline was infused into the trachea and gently recovered; this procedure was repeated four times and yielded approximately 4.5 ml lavage fluid. The cell-free bronchoalveolar lavage (BAL) fluids were concentrated 10-fold with a centrifugal filter (MWCO5000). The remaining lungs were cut into small pieces and homogenized in 10 mmol/L Hepes (pH 7.4). Small aliquots were saved as lung homogenate. The remaining homogenates were adjusted to 0.9 M sucrose/10 mmol/L Hepes (pH 7.4)/2 mmol/L $MgCl_2$ and layered on a 1.5 M sucrose cushion. Consecutive sucrose steps from 0.8 to 0.2 M were overlaid above the homogenate, and the discontinuous sucrose density gradients were centrifuged at 100,000 × *g* for 3 hours.[17,18] The 0.4 to 0.6 M layers were recovered as the lamellar body (LB) fraction. Protein concentrations were determined by deoxycholate-trichloroacetic acid precipitation and a bicinchoninic acid microprotein assay kit.

Fixed amounts of protein were subjected to 4% to 12% Bis-Tris SDS-polyacrylamide gel electrophoresis (PAGE) under reducing conditions and transferred to a nitrocellulose membrane. The membrane was immunoblotted with a rabbit anti-surfactant protein polyclonal antibody or a mouse anti-glyceraldehyde-3-phosphate dehydrogenase antibody, followed by a horseradish peroxidase-conjugated goat anti-rabbit (or goat anti-mouse) IgG antibody. The chemiluminescent detection assay was performed and exposed on an autofluorography film.

Phospholipid Assay

Male mice at 24 weeks old were used to prepare BAL fluids, lung homogenates, and lamellar body fractions. Total lipids were extracted according to the method of Bligh and Dyer.[19] In all samples, 20% of each sample was used for phospholipid phosphorus content determination with the method described by Bartlett.[20] The remaining 80% of each sample was used for two-dimensional thin-layer chromatography.[21] After development, the silica gel spot corresponding to phosphatidylcholine was scraped off and recovered quantitatively, and the phosphorus content quantified.

Triton X-114 Phase Separation of Mouse Lung Homogenates

Mouse lungs were cut into small pieces and homogenized in 10 mmol/L Hepes (pH 7.4) with a Potter-Elvehjem type homogenizer, followed by centrifugation at 300 × *g* for 10 minutes. The supernatant was divided into two equal aliquots. One aliquot (~0.5 ml) was centrifuged at 100,000 × *g* for 30 minutes. The volumes of the cytosolic and the pellet fractions were adjusted to be 0.5 ml. The second aliquot (~0.5 ml) was processed for Triton X-114 phase separation.[22] In brief, it was adjusted to 1% Triton X-114, rotated at 4°C for 2 hours, and centrifuged at 100,000 × *g* for 30 minutes. The supernatant was layered onto 6% sucrose/PBS/0.06% Triton X-114 in a 1.5 ml-microtube, and warmed up to 30°C for 10 minutes, followed by centrifugation at 300 × *g* for 10 minutes at room temperature. The upper layer was recovered as the aqueous phase. The oily droplet in the bottom was recovered as the detergent phase. The volumes of the two samples were adjusted to be equal (~0.5 ml). The equal volumes of aliquots (12.5 μl) were used for Western blotting.

Protein Production and Purification

The Rab38-cDNA originally cloned from a rat lung cDNA library was inserted into a pBlueBacHis-2A vector at BamHI and HindIII restriction enzyme sites. A forward primer that contains a BamHI restriction site and an initiation codon (5′-CCGGGATCCATGCAGACA-3′) and a reverse mutagenic PCR primer that carries the G146T-mutation site and adjacent HaeII restriction site (5′-GTAGCGCTTGATGATGCTGGTCTTGCCTACAACTA-3′) were used to amplify the sequence that contains the G146T mutation site. The PCR product was digested with BamHI and HaeII, and inserted into the pBlueBacHis-2A-Rab38 previously digested with BamHI and HaeII. Cationic liposomes were used to co-transfect the recombinant plasmid and a modified baculovirus DNA (Bac-N-Blue DNA) into Sf9 cells. Cells that were 80% to 90% confluent in 150-mm plastic dishes were infected with the

recombinant virus at a multiplicity of infection of 10, and cultured for 3 to 4 days. Ten to twenty plates of the infected Sf9 cells lysed in the lysis buffer (1% TritonX-114, 50 mmol/L Hepes, pH 7.4, 150 mmol/L NaCl, and 1.5 mmol/L EGTA) containing protease inhibitors (1 mmol/L PMSF, 10 μg/ml aprotinin, and 10 μg/ml leupeptin) were centrifuged at 100,000 $\times$ *g* for 30 minutes. The supernatant was loaded on a 2-ml bed volume of Ni^{++}-charged affinity column under native conditions. Imidazole step gradients were used to elute the column.

[^{32}P]GTP-Binding Assay

Between 0.5 and 1.5 μg of purified recombinant Rab38 was subjected to SDS-PAGE under reducing conditions. Subsequently, the proteins were electrophoretically transferred to a nitrocellulose membrane. [α-^{32}P]-GTP binding to the proteins immobilized on the membrane was determined.[23] The membrane was incubated with 60 nmol/L [α-^{32}P]-GTP [specific activity 3000Ci (111TBq)/mmol] (FP-208, Institute of Isotopes Co., Ltd., Budapest, Hungary) in 10 ml of Tris-HCl buffer for 1.5 hours at 25°C with gentle shaking on a platform shaker. The membrane was autoradiographed on an autoradiography film with an intensifying screen at −80°C for overnight. After development of the film, the membrane was washed with PBS and was probed by Western blotting with rabbit anti-rat Rab38 antibody (1:10,000)[5,7] for quantifying the amount of protein.

Immunoprecipitation of [^{3}H]-mevalonate-Radiolabeled Rab38

Sf9 cells were seeded at 3 $\times$ 10^6 cells/60-mm dish and infected with the recombinant baculovirus at a multiplicity of infection of 10 and cultured for 24 hours. Next, the cells were radiolabeled with 10 μCi/ml of [^{3}H]mevalonic acid (ART-334, ARC St. Louis, MO) in Grace's insect media with 10% fetal bovine serum (previously dialyzed against PBS) for 24 hours.[24] Ten μg/ml of mevinolin (Calbio 438186) was added 3 hours before adding radioisotope. The cells were lysed with 0.5 ml of 1% Triton X-100/PBS/5 mmol/L $MgCl_2$/antiproteases, followed by centrifugation at 100,000 $\times$ *g* for 30 minutes. A rabbit anti-rat Rab38 antibody[5,7] was added at ~4 μg/ml and the antigen-antibody complex was immunoprecipitated with 25-μl bed volume of protein A sepharose (CL-4B) beads (Sigma P-3391). The beads were eluted twice with 20 μl of 2$\times$ sample buffer containing 0.4 M dithiothreitol. This step typically yielded a total ~60 μl eluate sample. A 40 μl aliquot of the sample was used for autoradiography, and the remaining 20 μl was used for Western blot with a mouse anti-Xpress antibody (Invitrogen) for evaluation of the amount of immunoprecipitated Rab38.

Statistics

Data were expressed as mean ± SD. The data were evaluated by Student's *t*-test using Statview software (Abacus Concepts Inc, Berkley, CA), and $P < 0.05$ was considered statistically significant.

Results

Phenotype

In the C57BL/6J background, mice that are homozygous for chocolate (Rab38$^{cht/cht}$) have a rich dark brown coat instead of normal black coat (Figure 1A). Their skin pigmentation is also lighter, as can be seen in the ear and tail. Although we could not readily distinguish any eye color differences in these mutants, H&E staining of the eyeballs revealed a thinner pigment cell layer and choroid (Figure 1B). These mutant mice also showed a visible decrease in the melanin levels in their hair follicles. Hence, these animals exhibit an oculocutaneous albinism phenotype. We found no differences in the bleeding time between wild-type and chocolate mice at 12 weeks (data

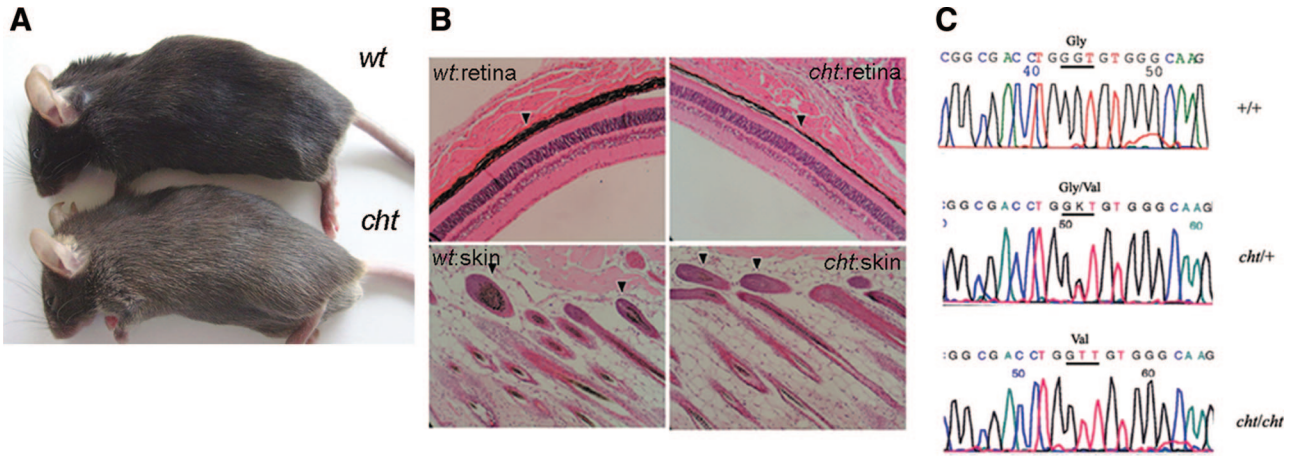

Figure 1. Chocolate mice show oculocutaneous albinism and harbor a point mutation in the Rab38 gene. **A:** An image of a wild-type (*wt*) C57BL/6J mouse (**upper**) and a mouse homozygous for the chocolate (*cht*) mutation (Rab38$^{cht/cht}$) in the same background (**lower**). The chocolate mouse develops a brown coat color and less pigmented skin around the ear and tail. **B:** Histology of the retina (**upper**) and the skin (**lower**). The chocolate mouse (**right**) shows a thinner pigment layer (**arrowhead**) in the retina and choroid, and reduced pigmentation in the hair follicles of the skin (**arrowhead**) compared with the wild-type mouse (**left**). **C:** A point mutation in exon 1 of the Rab38^{cht} gene, which contains the consensus GTP/GDP-interacting domain.

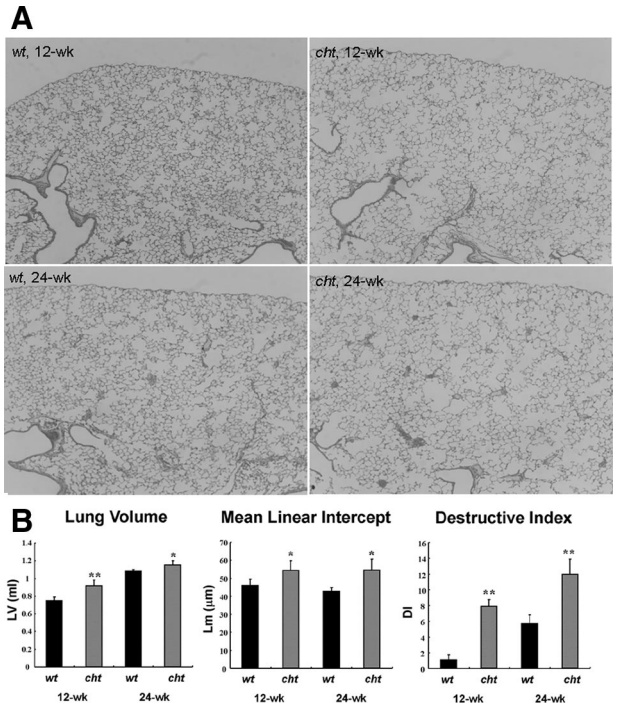

Figure 2. Chocolate mice develop aberrant lung structure. **A:** Lung histology. The mouse lungs were inflated with 2.5% glutaraldehyde via the trachea at + 25 cm H_2O pressure. Chocolate (*cht*) mice show an enlarged lower respiratory tract airspace compared with wild-type (*wt*) mice. H&E stain. Magnification = original ×20. **B:** Quantitative lung morphometry. The total lung volumes (LV), mean linear intercepts (Lm), and destructive indexes (DI) are significantly higher in chocolate mice, indicating that the chocolate lungs have enlarged distal airspace with more structural derangement compared with wild-type $n = 4$. $^*P < 0.05$, $^{**}P < 0.01$ *wt* vs. *cht* by unpaired Student's *t*-test. See Table 1 for details.

not shown), consistent with an earlier report.[9] The chocolate mice did not show any breeding or growth abnormalities during the 24 weeks observation period of our present study. No visible differences were evident between heterozygotes ($Rab38^{cht/+}$) and wild-type mice, confirming recessive nature of this phenotype. DNA sequencing of these mutants revealed a point mutation, G146T, in exon 1 of the Rab38 gene, which results in glycine to valine conversion (G19V) in the GTP/GDP-interacting domain of the encoded protein (Figure 1C).

Morphological Changes in the Lungs

Chocolate mice showed enlarged distal airspace in comparison with wild-type mice of the same age (Figure 2A). Based on the histological evaluation, no significant sign of inflammation was detected in the lung tissue sections. Total protein amounts and total cell numbers in the recovered BAL fluids were not significantly different between wild-type and chocolate mice (data not shown). In both groups, more than 96% of BAL cells were alveolar macrophages without any apparent difference in the appearance between the wild-type and the chocolate.

Lung volumes of chocolate mice measured by the water displacement were found to be significantly greater at both 12 and 24 weeks (Table 1, Figure 2B). In the mutant mice of both age groups, the volume proportion of the alveolar wall was significantly smaller, and the mean linear intercept was significantly larger compared with wild-type mice. At 24 weeks, the volume proportion of alveolar duct and sacs was significantly larger in the chocolate mice. The destructive index significantly increased in the mutant animals of both age groups and was observed to increase with age.

Toluidine-blue staining of the lung tissue of adult chocolate mice revealed the presence of alveolar type II cells with larger and more numerous cytoplasmic bodies than wild-type mice (Figure 3A). Electron microscopy demonstrated increased size and number of lamellar bodies, which completely filled cytoplasm of these cells from chocolate mice (Figure 3B). However, despite the increase in size and number of lamellar bodies in the mutant mice, they did not show any structural abnormalities. In contrast to the adult mice, 17-day fetal mice did not show apparent morphological difference in either alveolar type II cells or lamellar bodies when compared between wild-type and chocolate mice (Figure 3, C and D).

Pressure-Volume Relationship of the Lungs

Measurement of pressure-volume relationships was performed on the *in vivo* lungs in the open chests (Table 2). Lung volume at 25 cmH_2O airway pressure was significantly higher in chocolate mice than in wild-type mice. Static lung compliance was also significantly higher in chocolate mice. However, specific lung compliance, ie, static lung compliance divided by the lung volume at 25 cmH_2O airway pressure, was not significantly different. Neither airway opening pressure nor hysteresis ratio was significantly different between wild-type and mutant mice.

Table 1. Morphometric Analysis of Wild Type and Chocolate Mouse Lungs

12-week	*n*	LV	Vva	Vvd	Vvw	τw	Lm	la	ld	DI
12-week										
wt	4	0.75 ± 0.04	0.56 ± 0.04	0.24 ± 0.05	0.20 ± 0.02	4.44 ± 0.33	45.9 ± 3.5	37.4 ± 10.3	96.7 ± 25.0	1.1 ± 0.6
cht	4	0.92** ± 0.06	0.61 ± 0.04	0.23 ± 0.04	0.16* ± 0.01	4.25 ± 0.39	54.3* ± 5.5	29.5 ± 3.5	106.8 ± 20.1	7.9** ± 0.8
24-week										
wt	4	1.08 ± 0.02	0.64 ± 0.05	0.19 ± 0.03	0.17 ± 0.04	3.63 ± 0.68	42.7 ± 2.1	25.3 ± 2.4	111.9 ± 14.4	5.7 ± 1.0
cht	4	1.15* ± 0.05	0.60 ± 0.03	0.28** ± 0.03	0.11* ± 0.01	3.06 ± 0.10	54.5* ± 6.1	28.8 ± 2.6	129.4 ± 11.0	12.0** ± 1.9

Mean ± SD.

LV, lung volume (ml); Vva, volume proportion of alveoli; Vvd, volume proportion of alveolar ducts and sacs; Vvw, volume proportion of alveolar wall; τw, mean alveolar wall thickness (μm); Lm, mean linear intercept (μm); la, mean chord length of alveoli (μm); ld, mean chord length of ducts and sacs (μm); DI, destructive index.

$^*P < 0.05$, $^{**}P < 0.01$ *wt* vs. *cht* by unpaired Student's *t-test.*

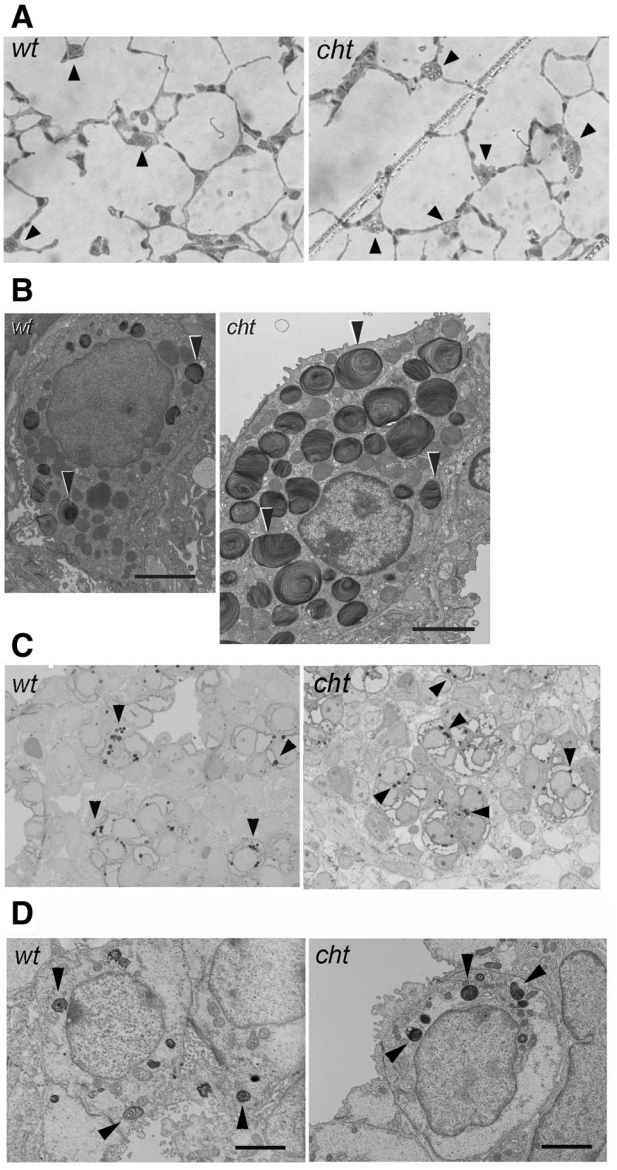

Figure 3. Alveolar type II cells in adult chocolate (*cht*) mice are enlarged and contain conspicuous lamellar bodies. In contrast, fetal mouse lungs do not show any apparent morphological difference in lamellar bodies. Lung pieces were fixed with 2% OsO_4/2.5% glutaraldehyde. **A, C:** 1% tolouidine blue stain of the 18 week-old mouse lungs (**A**) and 17-day fetal mouse lungs (**C**). Alveolar type II cells (**arrowhead**) in the adult chocolate mice were found to be enlarged and contain increased number of prominent, larger cytoplasmic vacuoles when compared with wild-type (*wt*) (**A**). Magnification = original ×200 (**A**), ×1000 (**C**). **B, D:** Electron microscopic appearance of alveolar type II cells. Lamellar bodies are indicated by **arrowheads**. The alveolar type II cells of the adult chocolate mice are enlarged and contain lamellar bodies of increased size in larger numbers (**B**). Scale bars = 2.5 μm. Magnification = original ×4000.

Abnormal Lung Surfactant Pooling in the Lung of Chocolate Mice

Lamellar bodies, lung homogenates, and BAL fluids from both wild-type and chocolate mice were analyzed by Western blotting for surfactant protein A (SP-A), surfactant protein B (SP-B), surfactant protein D (SP-D), and glyceraldehyde-3-phosphate dehydrogenase (GAPDH) by sequential immunoblotting and stripping of the same membrane. A representative result is shown in Figure 4A. SP-A was abundant in the BAL fluid, but no significant differences were evident between wild-type and chocolate mice. In contrast, SP-B was increased in the lung homogenate but decreased in the BAL fluid in chocolate mice. There was no difference in the BAL fluid SP-D. Although SP-A and SP-B appeared to be increased in the lamellar body fraction in chocolate mice, this was not statistically significant (Figure 4B). Phosphatidylcholine was increased in the lamellar body fraction and the lung homogenates in chocolate mice, but there was no difference in the BAL fluid. Total phospholipid levels in the samples of the lamellar body and the lung homogenate were also increased in chocolate mice but those in BAL fluids were equivalent (data not shown).

Characterization of Rab38^{cht} Protein

Native wild-type Rab38 protein was partitioned into both the aqueous and the detergent phases following Triton X-114 phase partitioning of mouse lung homogenates (Figure 5 left). This indicates the protein can have both hydrophilic and hydrophobic properties. Rab38 was found to exist in both membrane-bound and cytosolic form after a series of homogenization and centrifugation treatments of lung tissue (Figure 5 right). However, Rab38^{cht} mutant protein was exclusively partitioned into the aqueous phase and was only present in the cytosolic form. This result is consistent with the previous report of Rab38 in melanocytes derived from chocolate mice.[10] Thus, Rab38^{cht} is exclusively hydrophilic and unable to bind to membrane components *in vivo*.

Recombinant wild-type and mutant Rab38 proteins were generated using a baculovirus expression system in Sf9 cells, and were purified with a Ni^{++}-charged affinity column. Unexpectedly, when similar amounts of Rab38^{wt} and Rab38^{cht} proteins were subjected to Western transfer, these proteins showed equal binding capacities for [α-^{32}P]-GTP (Figure 6A). Next, Sf9 cells were infected with either of these two recombinant baculoviruses and cultured for 24 hours. These cells were radiolabeled with [^{3}H]-mevalonate in the presence of mevinolin and incubated for a further 24 hours. The cells were lysed and the resulting postnuclear supernatants were immunoprecipitated with a polyclonal rabbit anti-rat Rab38 antibody and protein A-sepharose beads. Although equal amounts of immunoreactive Rab38^{wt} and Rab38^{cht} proteins were obtained, Rab38^{cht}protein did not undergo posttranslational modification with [^{3}H]-mevalonate (Figure 6B). Thus, the mutant Rab38^{cht} protein failed to undergo post translational prenylation.

Discussion

This study is the first to demonstrate that chocolate mice exhibit abnormal lung surfactant homeostasis, conspicuous morphological changes of lamellar bodies, and de

Table 2. Pressure-Volume Analysis of Wild Type and Chocolate Mouse Lungs

	n	BW	V_{25}	V_{25}/BW	Paw	Cst	sCst	HR
wt	5	29.6 ± 2.7	1.01 ± 0.08	34.33 ± 4.13	4.78 ± 0.97	0.0446 ± 0.0048	0.0442 ± 0.0036	0.3066 ± 0.0197
cht	5	28.8 ± 3.7	1.29** ± 0.11	45.18* ± 6.02	5.98 ± 2.69	0.0525* ± 0.0053	0.0409 ± 0.0042	0.348 ± 0.063

Mean ± SD. Mice at 24 weeks-old were used.
BW, body weight (g); V_{25} , Lung volume at 25cmH_2O airway pressure (ml); Paw, airway opening pressure (cmH_2O); Cst, static lung compliance (ml/cmH_2O); sCst, specific lung compliance (ml/cmH_2O/ml); HR, hysteresis ratio.
*$P < 0.05$, **$P < 0.01$ *wt* vs. *cht* by unpaired Student's t-test.

velop lung structural abnormalities, in addition to the previously described oculocutaneous albinism. The molecular basis for the phenotype is defective membrane-binding activity of Rab38^{cht} due to failure of prenyl modification, but not loss of GTP-binding activity.

The recombinant Rab38^{cht} protein was unexpectedly found to retain an efficient level of GTP-binding activity, even though the amino acid mutation itself (G19V) was in the conserved GTP/GDP-interacting domain near N-terminus of the native protein.[9] Although not an invariant residue within Rab family, glycine 19 is conserved in >50% of Rab proteins. The corresponding amino acid in Rab5 is alanine 30. The fact that a Rab5 A30V mutant shows increased GTP-binding activity[25] is consistent with our unexpected finding for Rab38^{cht} (Figure 6A). Although Rab38^{cht} protein retains its GTP-binding activity, it is not bound to any membrane components (Figure 5). The inability of unprenylated mutant Rab38 to bind to the required membrane components appears to cause its loss of biological activity, as this phenomenon was demonstrated previously for other small GTPase mutants.[26] The precise mechanism underlying the failure of the mutant protein to undergo prenylation is currently unknown. It is possible that the mutant cannot interact normally with either the Rab escort protein or Rab geranylgeranyl transferase, and is thereby unavailable for prenyl modification.

We hypothesized that abrogation of Rab38 function would affect the lungs as well as the skin because the mRNA and protein expression levels are highest in this organ.[7] Chocolate mice developed aberrant alveolar structures: increased mean linear intercept, destructive index, and volume proportion of alveolar ducts and sacs; and decreased volume proportion of alveolar walls (Figure 2, Table 1). However, these morphological changes were mild and not comparable with lung emphysema in cigarette smoke-exposed mice[27] or SP-D knockout

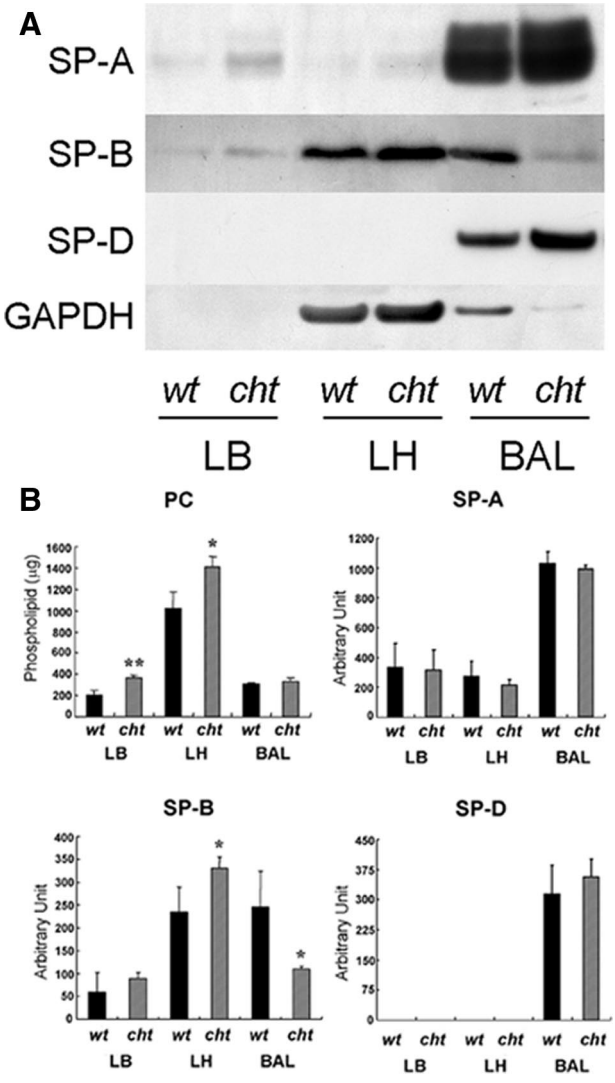

Figure 4. Lung surfactant accumulates in alveolar type II cells but not in the alveolar lumen of chocolate mice. **A:** Western blot analysis of three surfactant apoproteins SP-A, SP-B, and SP-D. The same blot was sequentially stripped and incubated with four different primary antibodies and the corresponding secondary antibodies. The protein loading amounts were 1 μg for lamellar bodies (LB), 50 μg for lung homogenate (LH), and 10 μg for bronchoalveolar lavage (BAL) fluid. **B:** Statistical analysis of phosphatidylcholine (PC) and surfactant apoprotein levels (SP-A, SP-B, and SP-D). PC was measured using two-dimensional thin layer chromatography. The intensities of the SP-A, -B, and -D signals detected by Western blotting were determined by densitometry. $n = 3$. *$P < 0.05$, **$P < 0.01$ *wt* vs. *cht* by unpaired Student's *t*-test.

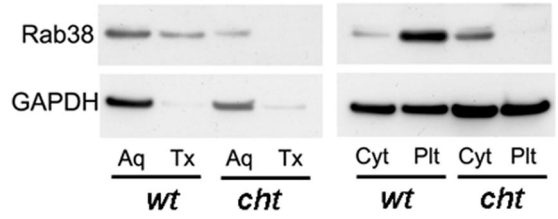

Figure 5. Native Rab38^{cht} proteins are partitioned into the aqueous phase and are not bound to membrane components. Mouse lungs were homogenized and centrifuged at 300 × *g* for 10 minutes. The supernatant was then recovered as postnuclear supernatant. **Left:** Triton X-114 was added to a final concentration of 1% and phase partitioning was performed. **Right:** The postnuclear supernatant was further centrifuged at 100,000 × *g* for 30 minutes, and recovered as a cytosolic fraction and a membrane pellet fraction. Equivalent amount of samples were processed for Western blotting using a rabbit anti-Rab38 as the primary antibody. Aq = aqueous phase. Tx = detergent phase. Cyt = cytosolic fraction. Plt = membrane pellet fraction.

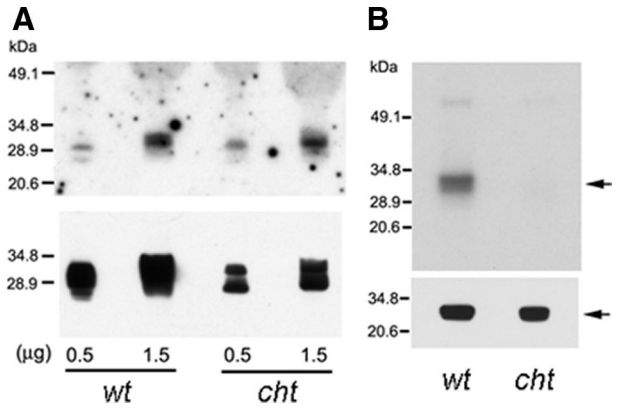

Figure 6. Rab38^{cbt} proteins retain GTP-binding activity but do not undergo prenyl modification. **A:** (**Upper**) The recombinant proteins were produced in Sf9 cells infected with recombinant baculovirus expressing wild-type or mutant Rab38, purified with a Ni^{++}-affinity column, and subjected to SDS-PAGE and transferred to a nitrocellulose membrane. The membrane was incubated with [α-^{32}P]-GTP and autoradiographed. (**Lower**) The same membrane was then immunoblotted with a rabbit anti-Rab38 antibody. **B:** Sf9 cells infected with recombinant baculovirus expressing wild-type or mutant Rab38 (**arrows**) were radiolabeled with [^{3}H]-mevalonate in the presence of mevinolin. The recombinant proteins were immunoprecipitated with a rabbit anti-rat Rab38 antibody and protein A-sepharose beads. (**Upper**) One aliquot of the immunoprecipitated antigen-antibody complexes was used for SDS-PAGE and autoradiofluorography. (**Lower**) The other aliquot was analyzed by Western blotting with a mouse anti-Xpress antibody to quantify the immunoprecipitated Rab38 levels.

mice.[28] Physiological analysis showed that the chocolate lungs have slightly increased lung compliance, but the difference was abolished after dividing by lung volume, ie, specific lung compliance. This result suggests that chocolate mice have hyperinflationary lungs rather than emphysematous lungs with prominent alveolar destruction. No apparent sign of inflammation was observed in BAL fluids or in the lung tissues in chocolate mice (data not shown). Thus, it is likely that alveolar structural changes in chocolate mice were caused by developmental abnormality rather than inflammatory tissue derangement. However, precise mechanism for development of these alveolar structural abnormalities remains undefined.

Lung surfactant is a complex of several lipids (mainly phosphatidylcholine) and four surfactant apoproteins, SP-A, -B, -C, and -D.[29] With the exception of SP-D, these surfactant components are stored in lamellar bodies in alveolar type II cells. Accumulating evidences suggest different intracellular transport pathways for each surfactant component. Newly synthesized phosphatidylcholine is transported to and stored in lamellar bodies via a Golgi-independent pathway.[17] Newly synthesized SP-A is transported to the Golgi apparatus and undergoes glycosylation and is then secreted. A portion of the secreted SP-A is subsequently transported into lamellar bodies.[18] Newly synthesized SP-B is also transported to the Golgi apparatus, and then to the lamellar bodies to be stored.[30] SP-D is synthesized and transported to the Golgi apparatus, and then secreted, but is not routed to the lamellar bodies.[31] Both SP-A- and SP-D-deficient mice contain lamellar body organelles in their alveolar type II cells.[32,33] Hence, phosphatidylcholine and SP-B appear to be closely associated with biogenesis of lamellar bodies, although the molecular details are not yet fully understood. Given the fact that chocolate alveolar type II cells contain numerous enlarged lamellar bodies, and that phosphatidylcholine and SP-B levels are increased in the cells but not in the BAL fluid, it is likely that the secretory machinery of lamellar bodies that store phosphatidylcholine and SP-B is defective in mutant cells as a consequence of dysfunctional Rab38 protein.

Oculocutaneous albinism and lung disease are closely related to Hermansky-Pudlak syndrome (HPS). HPS is clinically characterized by oculocutaneous albinism, bleeding diathesis, and life-limiting pulmonary fibrosis, although the clinical presentation is heterogeneous.[34] The most critical problem for patients with HPS is lung fibrosis, which may lead to death between the fourth and fifth decade of life.[34–36] HPS is an autosomal recessive disease resulting from heterogeneous genetic abnormalities.[35] Eight genetically distinct forms of HPS have so far been identified in humans (HPS1–8). Most of the mutant genetic products involved in these variant forms of HPS participate in vesicle trafficking that regulates biogenesis of lysosome-related organelles.[37] There is accumulating evidence that Rab38 is involved in biogenesis of melanosomes in skin melanocytes and retinal pigment epithelial cells.[9–11] Given their high expression of Rab38, there could be a possible link between melanocytes and alveolar type II cells, in which their characteristic cell organelles may be involved. Both cells contain lysosome-related organelles that consist of melanosomes in melanocytes, and lamellar bodies in alveolar type II cells. Lamellar bodies are lung surfactant storage granules and lysosome-related organelles.[38]

The observed lung changes in chocolate mice are similar to those reported in the mouse homologues of human HPS, *pale ear* (*ep*), *pearl* (*pe*), and the double mutant *ep/ep*, *pe/pe*.[39] However, each strain develops emphysematous lung disease instead of pulmonary fibrosis. The discrepancy between mouse and human in the homologous genetic abnormality are not clear. However, recent studies show that HPS mice are more susceptible to bleomycin-induced pulmonary fibrosis than wild-type mice.[40] Different environmental conditions between mice and humans may be associated with the phenotype discrepancy. The double mutant *ep/ep, pe/pe* mice show integrated lung changes with striking abnormalities in alveolar type II cells and share some lung pathological features with human HPS. As seen in the chocolate lungs, alveolar type II cells and lamellar bodies are remarkably enlarged, and lamellar bodies are engorged with surfactant. In the case of the double mutant mice, airspaces of the mutant lungs contain age-related elevations in the numbers of inflammatory cells and foamy macrophages. These features were also shown in the lung pathology of HPS patients.[41]

In rats, two (Hermansky-Pudlak Syndrome) animal models have been described: Fawn-Hooded rats and Tester-Moriyama rats. Fawn-Hooded rats develop several diseases including oculocutaneous albinism, bleeding diathesis, pulmonary hypertension, systemic hypertension, renal failure, depression, and alcoholism.[42] The

oculocutaneous albinism and bleeding diathesis that manifests in Fawn-Hooded rats has been attributed to the pleiotropic effects of a single locus, *Ruby* (*R*). Recently, the *Ruby* locus was identified as the *Rab38* gene, establishing that rat *Ruby* and mouse chocolate genes are homologues.[43] However, chocolate mice lack platelet storage granule deficiency and subsequent bleeding diathesis. One possible explanation for this is that as the Rab38^{cht} mutant is a full length protein, it can still facilitate platelet storage granules to be formed and secreted. In contrast, the Rab38 Met1Ile substitution found in both Fawn-Hooded and Tester-Moriyama rats is a protein-null defect, as it completely abolishes translation from the mutant allele. It is possible that a complete deficit of Rab38 causes a platelet pool storage deficiency and a prolonged bleeding time.

In summary, Rab38^{cht}-mutant mice develop an abnormal lung phenotype as well as oculocutaneous albinism due to altered homeostasis of systemic lysosome-related organelles. We suggested that genetic abnormality of human Rab38 may also cause the phenotype of HPS in humans.

Acknowledgments

The authors thank Ms. Maki Sakuta and Ms. Tomoko Miwa for their technical assistance.

References

1. Takai Y, Sasaki T, Matozaki T: Small GTP-binding proteins. Physiol Rev 2001, 81:153–208
2. Zerial M, McBride H: Rab proteins as membrane organizers. Nat Rev Mol Cell Biol 2001, 2:107–117
3. Seabra MC, Wasmeier C: Controlling the location and activation of Rab GTPases. Curr Opin Cell Biol 2004, 16:451–457
4. Pfeffer S, Aivazian D: Targeting Rab GTPases to distinct membrane compartments. Nat Rev Mol Cell Biol 2004, 5:886–896
5. Osanai K, Iguchi M, Takahashi K, Nambu Y, Sakuma T, Toga H, Ohya N, Shimizu H, Fisher JH, Voelker DR: Expression and localization of a novel Rab small G protein (Rab38) in the rat lung. Am J Pathol 2001, 158:1665–1675
6. Jager D, Stockert E, Jager E, Gure AO, Scanlan MJ, Knuth A, Old LJ, Chen YT: Serological cloning of a melanocyte rab guanosine 5′-triphosphate-binding protein and a chromosome condensation protein from a melanoma complementary DNA library. Cancer Res 2000, 60:3584–3591
7. Osanai K, Takahashi K, Nakamura K, Takahashi M, Ishigaki M, Sakuma T, Toga H, Suzuki T, Voelker DR: Expression and characterization of Rab38, a new member of the Rab small G protein family. Biol Chem 2005, 386:143–153
8. MacPikeA, Mobraaten LE: New coat color mutations. Dbr and cht Mouse News Lett 1984, 70:86
9. Loftus SK, Larson DM, Baxter LL, Antonellis A, Chen Y, Wu X, Jiang Y, Bittner M, Hammer JA 3rd, Pavan WJ: Mutation of melanosome protein RAB38 in chocolate mice. Proc Natl Acad Sci USA 2002, 99:4471–4476
10. Wasmeier C, Romao M, Plowright L, Bennett DC, Raposo G, Seabra MC: Rab38 and Rab32 control post-Golgi trafficking of melanogenic enzymes. J Cell Biol 2006, 175:271–281
11. Lopes VS, Wasmeier C, Seabra MC, Futter CE: Melanosome maturation defect in Rab38-deficient retinal pigment epithelium results in instability of immature melanosomes during transient melanogenesis. Mol Biol Cell 2007, 18:3914–3927
12. Weibel ER. Stereological methods, vol. 1: Practical methods for biological morphometry. New York, Academic Press 1979, pp. 30–161
13. Kawakami M, Paul JL, Thurlbeck WM: The effect of age on lung structure in male BALB/cNNia inbred mice. Am J Anat 1984, 170:1–21
14. Saetta M, Shiner RJ, Angus GE, Kim WD, Wang NS, King M, Ghezzo H, Cosio MG: Destructive index: a measurement of lung parenchymal destruction in smokers. Am Rev Respir Dis 1985, 131:764–769
15. Saito K, Cagle P, Berend N, Thurlbeck WM: The "destructive index" in nonemphysematous and emphysematous lungs. Morphologic observations and correlation with function. Am Rev Respir Dis 1989, 139:308–312
16. Nardell EA, Brody JS: Determinants of mechanical properties of rat lung during postnatal development. J Appl Physiol 1982, 53:140–148
17. Osanai K, Mason RJ, Voelker DR: Pulmonary surfactant phosphatidylcholine transport bypasses the brefeldin A sensitive compartment of alveolar type II cells. Biochim Biophys Acta 2001, 1531:222–229
18. Osanai K, Mason RJ, Voelker DR: Trafficking of newly synthesized surfactant protein A in isolated rat alveolar type II cells. Am J Respir Cell Mol Biol 1998, 19:929–935
19. Bligh EG, Dyer WJ: A rapid method of total lipid extraction and purification. Can J Biochem Physiol 1959, 37:911–917
20. Bartlett GR: Phosphorus assay in column chromatography. J Biol Chem 1959, 234:466–468
21. Poorthuis BJ, Yazaki PJ, Hostetler KY: An improved two dimensional thin-layer chromatography system for the separation of phosphatidylglycerol and its derivatives. J Lipid Res 1976, 17:433–437
22. Bordier C: Phase separation of integral membrane proteins in Triton X-114 solution. J Biol Chem 1981, 256:1604–1607
23. Lapetina EG, Reep BR: Specific binding of [α-^{32}P]GTP to cytosolic and membrane-bound proteins of human platelets correlates with the activation of phospholipase C. Proc Natl Acad Sci USA 1987, 84:2261–2265
24. Page MJ, Hall A, Rhodes S, Skinner RH, Murphy V, Sydenham M, Lowe PN: Expression and characterization of the Ha-ras p21 protein produced at high levels in the insect/baculovirus system. J Biol Chem 1989, 264:19147–19154
25. Li G, Liang Z: Phosphate-binding loop and Rab GTPase function: mutations at Ser29 and Ala30 of Rab5 lead to loss-of-function as well as gain-of-function phenotype. Biochem J 2001, 355:681–689
26. Hancock JF, Magee AI, Childs JE, Marshall CJ: All ras proteins are polyisoprenylated but only some are palmitoylated. Cell 1989, 57:1167–1177
27. Sato T, Seyama K, Sato Y, Mori H, Souma S, Akiyoshi T, Kodama Y, Mori T, Goto S, Takahashi K, Fukuchi Y, Maruyama N, Ishigami A: Senescence marker protein-30 protects mice lungs from oxidative stress, aging, and smoking. Am J Respir Crit Care Med 2006, 174:530–537
28. Wert SE, Yoshida M, LeVine AM, Ikegami M, Jones T, Ross GF, Fisher JH, Korfhagen TR, Whitsett JA: Increased metalloproteinase activity, oxidant production, and emphysema in surfactant protein D gene-inactivated mice. Proc Natl Acad Sci USA 2000, 97:5972–5977
29. Goerke J: Pulmonary surfactant: functions and molecular composition. Biochim Biophys Acta 1998, 1408:79–89
30. Korimilli A, Gonzales LW, Guttentag SH: Intracellular localization of processing events in human surfactant protein B biosynthesis. J Biol Chem 2000, 275:8672–8679
31. Gobran LI, Rooney SA: Regulation of SP-B and SP-C secretion in rat type II cells in primary culture. Am J Physiol Lung Cell Mol Physiol 2001, 281:L1413–L1419
32. Korfhagen TR, Bruno MD, Ross GF, Huelsman KM, Ikegami M, Jobe AH, Wert SE, Stripp BR, Morris RE, Glasser SW, Bachurski CJ, Iwamoto HS, Whitsett JA: Altered surfactant function and structure in SP-A gene targeted mice. Proc Natl Acad Sci USA: 1996, 93:9594–9599
33. Botas C, Poulain F, Akiyama J, Brown C, Allen L, Goerke J, Clements J, Carlson E, Gillespie AM, Epstein C, Hawgood S: Altered surfactant homeostasis and alveolar type II cell morphology in mice lacking surfactant protein D. Proc Natl Acad Sci USA 1998, 95:11869–11874
34. Huizing M, Anikster Y, Gahl WA: Hermansky-Pudlak syndrome and related disorders of organelle formation. Traffic 2000, 1:823–835
35. Di Pietro SM, Dell'Angelica EC: The cell biology of Hermansky-Pudlak syndrome: recent advances. Traffic 2005, 6:525–533
36. Gahl WA, Brantly M, Troendle J, Avila NA, Padua A, Montalvo C, Cardona H, Calis KA, Gochuico B: Effect of pirfenidone on the pulmonary fibrosis of Hermansky-Pudlak syndrome. Mol Genet Metab 2002, 76:234–242
37. Dell'Angelica EC: The building BLOC (k) s of lysosomes and related organelles. Curr Opin Cell Biol 2004, 16:458–464
38. Weaver TE, Na CL, Stahlman M: Biogenesis of lamellar bodies, lyso-

some-related organelles involved in storage and secretion of pulmonary surfactant. Semin Cell Dev Biol 2002, 13:263–270
39. Lyerla TA, Rusiniak ME, Borchers M, Jahreis G, Tan J, Ohtake P, Novak EK, Swank RT: Aberrant lung structure, composition, and function in a murine model of Hermansky-Pudlak syndrome. Am J Physiol Lung Cell Mol Physiol 2003, 285:L643–L653
40. Young LR, Pasula R, Gulleman PM, Deutsch GH, McCormack FX: Susceptibility of Hermansky-Pudlak mice to bleomycin-induced type II cell apoptosis and fibrosis. Am J Respir Cell Mol Biol 2007, 37:67–74
41. Nakatani Y, Nakamura N, Sano J, Inayama Y, Kawano N, Yamanaka S, Miyagi Y, Nagashima Y, Ohbayashi C, Mizushima M, Manabe T, Kuroda M, Yokoi T, Matsubara O: Interstitial pneumonia in Hermansky-Pudlak syndrome: significance of florid foamy swelling/degeneration (giant lamellar body degeneration) of type-2 pneumocytes. Virchows Arch 2000, 437:304–313
42. Prieur DJ, Meyers KM: Genetics of the fawn-hooded rat strain. The coat color dilution and platelet storage pool deficiency are pleiotropic effects of the autosomal recessive red-eyed dilution gene. J Hered 1984, 75:349–352
43. Oiso N, Riddle SR, Serikawa T, Kuramoto T, Spritz RA: The rat Ruby (*R*) locus is Rab38: identical mutations in Fawn-hooded and Tester-Moriyama rats derived from an ancestral Long Evans rat sub-strain. Mamm Genome 2004, 15:307–314